

The Problem of Cosmogenic Activation in Double Beta Decay Experiments

Susana Cebrián

Laboratorio de Física Nuclear y Altas Energías

Universidad de Zaragoza. 50009 Zaragoza

Premio a la Investigación de la Academia. 2004

Abstract

Large efforts are being devoted to the detection of the neutrinoless nuclear double beta decay since this process is a probe to investigate the lepton number violation and the Dirac or Majorana nature of the neutrino, as well as to measure the absolute scale of the neutrino mass spectrum. Since double beta decay is a rare process, experiments with an ultra-low background are mandatory to attempt its detection; for this reason, double beta decay experiments are installed in underground laboratories. Activity induced in detectors and materials of the experimental set-up by the exposure to cosmic rays when being above ground gives a significant contribution to the background. The main difficulty to study quantitatively the problem of cosmic activation in double beta decay experiments is the lack of accurate information (either from measurements or from calculations) on the cross-sections of isotope production in the targets of interest. Here, an overview of data libraries and computational codes (following different approaches) to be used in these studies of cosmogenic activation is given. Results on isotope production cross sections for the particular case of germanium detectors have been collected and elaborated; for the production of ^{68}Ge in ^{76}Ge (the most relevant pair of product-target in enriched germanium detectors) differences from the several estimates reach up to a factor ~ 50 . It can be concluded that experimental measurements of production cross sections in the specific targets of interest for Double Beta Decay and further development on models and codes are still necessary to be able to make accurate estimates of activation yields.

1 Introduction

Neutrinoless Double Beta Decay (DBD) consists of the direct emission of two electrons from a nucleus (A,Z) decaying to the corresponding isobar $(A,Z+2)$. This process can be searched for when the single beta transition from (A,Z) to $(A,Z+1)$ is energetically forbidden or at least strongly hindered by a large change of the spin-parity state. The standard process of DBD is accompanied by the emission of two electron anti-neutrinos and therefore conserves lepton number. It is allowed by the standard model of electroweak interactions, and it has been found in ten nuclei. On the contrary, conservation of the lepton number is violated in neutrinoless DBD and in the majoron decay, where the massless Goldstone boson accompanies the emission of the two electrons. In neutrinoless channel, these two particles would share the total transition energy and a peak would appear in the sum energy spectrum of the two electrons. In addition, the available phase space is much larger with respect to the two neutrino one, rendering neutrinoless DBD a very powerful way to search for lepton number non-conservation.

Strong interest has been revived in the field of double beta decay (DBD) by the recent discovery of neutrino oscillations in solar [1, 2], atmospheric [3], and reactor [4] experiments. This discovery indicates a non-zero value for the difference between two neutrino mass eigenvalues. It becomes therefore imperative to search for a finite value for the effective electron neutrino mass [5]. The study of neutrinoless DBD can shed light on the neutrino nature (Dirac or Majorana particle) as well as on the absolute neutrino mass scale, since the half-life for the neutrinoless DBD mode is

$$T_{1/2}^{0\nu} \propto \frac{\langle m_\nu \rangle^2}{m_e^2}$$

being the parameter

$$\langle m_\nu \rangle = \sum_j \lambda_j m_j U_{ej}^2$$

the so-called neutrino effective mass, with U_{ej} the matrix describing the mixing between the electron neutrino and the neutrino mass eigenstates m_j and λ_j a phase factor related to CP conservation. Present DBD searches explore the neutrino mass scale in the 0.2 - 0.5 eV range (see Ref. [6]). Innovative techniques in experiments of next generation seem capable to extend the neutrino Majorana mass sensitivity down to ~ 0.05 - 0.01 eV.

In astrophysics, the recent results of the full sky microwave maps by WMAP together with the 2dF galaxy redshift survey [7] constrain to less than eV the sum of the masses of neutrinos of the three flavors. Direct experiments on single beta decay presently constrain the absolute value of this mass to less than 2.2 eV, while a bound of 0.2 eV is expected in the KATRIN experiment [8]. A more restrictive limit for the effective mass of Majorana

neutrinos can undoubtedly come from neutrinoless double beta decay.

Experiments devoted to the direct search for neutrinoless DBD are based on two different approaches. In the source \neq detector one, thin sheets of a double beta active material are inserted in a suitable detector. In the source=detector or “calorimetric” experiments [9] the detector itself is made of a material containing the double beta active nucleus. Detectors should measure the energy deposited by electrons emitted in the DBD process (a peak at the transition energy in the case of neutrinoless DBD).

No evidence has been confirmed so far for the neutrinoless channel in any nucleus. An alleged evidence for neutrinoless DBD of ^{76}Ge was reported in 2001 by a subset of the Heidelberg–Moscow Collaboration [10], but confronted by other authors [11], and even by a different subset of the same collaboration [12]. More recently, adding statistics and making a new analysis of all the data, an indication of neutrinoless DBD of ^{76}Ge is claimed by the authors at a confidence level of 4.2σ [13]. Theoretical aspects, experimental approaches and results regarding DBD can be found in recent reviews of the field [6].

The half-lives of DBD emitters are of the order of $10^{20} - 10^{25}$ years, that is, DBD is a very rare process. For this reason, an ultra-low background is required in detectors aiming to detect the DBD signal. The contribution of cosmic rays is almost suppressed in this kind of experiments installing them in very deep underground laboratories, while environmental backgrounds (radon, neutrons, U/Th radioactivity, potassium, ...) can be reduced using active and passive shieldings [14]. Consequently, intrinsic radioactive impurities in materials of the experimental set-up, like cosmogenic activity induced at sea level, may become a serious problem. The main difficulty for studying quantitatively the problem of cosmogenic activation is the lack of accurate information on the isotope production cross sections for the targets of interest in DBD.

The goal of this work is to provide an overview of data sources and available codes to be used in studies of cosmogenic activation for particular DBD experiments. This information can be also useful in the background studies of experiments devoted to the search for other rare events, like the interaction of Weakly Interacting Massive Particles (WIMPs) which can constitute the dark matter of the galactic halo. The presentation of the work is organized in the following way. In Section 2, some basic concepts of cosmogenic activation are presented. In Section 3, the results of examining various nuclear data libraries following different approaches in the search for production cross sections in targets of interest are shown. Section 4 presents some of the computational codes which can be used in activation studies, focusing on the underlying physics and the advantages and disadvantages for their use in the field of DBD. In Section 5, different results for cosmogenic isotope production cross sections in germanium, from libraries and calculations described in the previous sections, are discussed. Germanium has been chosen since it is the preferred detector material in many DBD projects.

2 Cosmogenic activation

Radioactivity in the environment can be natural (formed in stellar evolutionary processes and captured in the formation of the Earth), man-made (produced by fusion, fission, accelerator reactions, . . .) or cosmogenically induced. One of the most relevant cosmogenic processes is the spallation of nuclei by high energy neutrons (activation by primary cosmic radiations like protons or alpha particles is negligible since most of these particles are absorbed by the atmosphere). Cosmogenic radioactivity is mostly produced in the atmosphere, but measurable amounts occur also at the surface of the Earth. At the Earth's surface, nuclide production is dominated by neutrons ($\sim 95\%$) making protons only a minor contribution ($\sim 5\%$). For the reactions of cosmogenic production of a certain isotope, the cross section decreases and the energy threshold of the process increases with the difference between the mass numbers (ΔA) of the target and product nuclides.

The production rate R of an isotope with constant decay λ by exposure to cosmic neutrons is calculated as:

$$\int \sigma(E)\phi(E)dE$$

being σ the cross-section for the production, ϕ the flux of neutrons and E the neutron energy. For a exposure time t_{expo} , the induced activity A is:

$$A = R(1 - \exp(-\lambda/t_{expo}))$$

Consequently, to estimate the cosmogenic induced activity in a material there are three basic ingredients: the history of the material (time of exposure at sea level, if it has flown or been stored underground, . . .), the flux of cosmic rays and the cross-section of isotope production. Cross-sections are undoubtedly the element which introduce the biggest uncertainties in activation studies; therefore, attention must be primarily paid to them.

The cosmic ray neutron flux spectra frequently employed in cosmogenic studies for DBD are taken from the works of Lal & Peters [15] and of Hess [16]. Differences are noticeable for high energy neutrons (above ~ 200 MeV), which affects the production rates significantly for reactions with high threshold energies. A more recent compilation of the neutron flux spectrum, including relevant corrections to the traditional spectra, is given in [17]; the use of this spectrum should give more reliable results. The effect of altitude and latitude on the neutron flux is also discussed in this work.

Since DBD requires ultra-low background experiments, the understanding of the effect of exposing detectors to cosmic ray neutrons is very important. It is worth noting that this background contribution cannot be removed afterwards, being a very important intrinsic impurity for the detector material itself. The dominant mechanism for activation in DBD experiments is by energetic neutron spallation reactions. Although detectors used for this

kind of experiments are installed underground, which strongly reduces the cosmic ray flux, activation can take place when materials are on surface (for fabrication, transport, storage, ...). If detectors are flown to high altitudes, in addition to the fact that the cosmic ray neutron flux may be two orders of magnitude greater than at sea level, there may be a measurable effect from protons as well.

The only way to avoid cosmic activation of materials is keeping them in a proper shielding against the hadronic component of the cosmic rays. Flying must be avoided and the exposure time on the surface of the Earth should be kept as small as possible. Since these requirements usually complicate the preparation of experiments, it would be very useful to have reliable tools to quantify accurately the real danger of exposing the materials to cosmic rays.

Just to have an idea of the present status of cosmogenic activation studies in the field of DBD, Table 1 summarizes the main features of the studies carried out for different projects and experiments. They are based on different codes (which will be presented later on), like a modified version of COSMO, Σ , ISABEL, and GEANT4. Despite the fact that the uncertainties in the results are known to be large, no cross-check is usually presented using different codes. The activation studies have been applied basically to the detector material, specially germanium, and in some cases, for some other relevant materials in the experimental set-up like copper or nitrogen.

Table 1.— Main features of the activation studies carried out for different projects and DBD experiments.

Experiment /Project	Target	Code	Reference
Majorana	Ge, Cu	ISABEL, [18]	[19]
CUORE	TeO ₂	Modified COSMO	[20]
GENIUS	Ge, N ₂	Σ	[21]
GERDA	Ge	[18]	[22]
Heidelberg /Moscow	Ge	Σ , GEANT4	[23]
NUSL	Ge, Cu	Modified COSMO	[24]

3 Data from libraries

In this section available information on cross sections for isotope production induced by bombarding targets of interest in DBD experiments with neutrons and protons is collected from different nuclear data libraries. Four data libraries, based on different approaches, have been examined.

3.1 EXFOR

EXFOR experimental nuclear reaction data library (in USA usually called CSISRS) [25] contains data compiled as the result of the cooperative efforts of the world-wide Nuclear Reaction Data Center network which is coordinated by the International Atomic Energy Agency (IAEA) Nuclear Data Section. The neutron data part of EXFOR is relatively complete due to the long history of neutron data compilation activities. In particular, the data for incident neutrons below 20 MeV energy are assumed to be complete. The charged particle and photonuclear data contained in this library are not so comprehensive because of the much smaller and more intermittent support given to the compilation of such data. The EXFOR retrieval web page [25] gives easy access to the data. The user should specify a particular reaction (inelastic scattering, (n,γ) , (n,p) , (n,t) , ...), or a desired residual nucleus and projectile, and the program will generate a list of data sets which satisfy the retrieval criteria. Cross sections for (n,X) processes in all isotopes in natural germanium and tellurium¹ when bombarded by neutrons and protons have been searched; Table 2 shows the unique cases with a positive output. This information, even if not directly useful for the activation studies in DBD experiments, can be very precious to check the reliability of codes developed to determine relevant production cross sections since EXFOR gives only results from measurements.

Table 2.— Reactions for which data are available from the EXFOR data base for germanium and tellurium isotopes bombarded by protons or neutrons.

target	projectile	products
⁷⁰ Ge	p	⁶⁹ Ge
¹²² Te	p	¹¹⁸ Te, ¹¹⁹ Te
¹²³ Te	p	¹¹⁸ Te, ¹¹⁹ Te
¹³⁰ Te	p	⁶⁶ Ge, ⁶⁷ Ge, ⁶⁹ Ge, ⁷⁵ Ge, ⁷⁷ Ge, ⁷⁹ Ge, ^{69–72} As, ⁷⁴ As, ⁷⁶ As, ⁷⁸ As, ⁷⁹ As
¹²⁸ Te	n	¹²⁷ Sb
¹²³ Te	n	¹²² Sb

3.2 RNAL

RNAL (Reference Neutron Activation Library) [26] is a library of evaluated cross sections for neutron induced reactions leading to radioactive products. These reactions are used in various applications, especially in the activation analysis. The evaluations

¹The isotopic composition of natural germanium is: ⁷⁰Ge 20.84%, ⁷²Ge 27.54%, ⁷³Ge 7.73%, ⁷⁴Ge 36.28%, and ⁷⁶Ge 7.61%. The isotopic composition of natural tellurium is: ¹²⁰Te 0.09%, ¹²²Te 2.55%, ¹²³Te 0.89%, ¹²⁴Te 4.74%, ¹²⁵Te 7.07%, ¹²⁶Te 18.84%, ¹²⁸Te 31.74%, and ¹³⁰Te 34.08%.

have been selected from various national and regional projects and assembled at IAEA Nuclear Data Section. The standard ENDF-6 (Evaluated Nuclear Data File) format is used.

The library is restricted to 255 important reactions, which are listed in Table 6 in Appendix A. The relatively small number of reactions allowed for a detailed assessment of the library providing the user with the information on the quality of the data.

Unfortunately, most of the reactions considered in this library do not have interest for activation in DBD and a too limited number of processes is studied. No reaction for activation in germanium isotopes is included. Cross-sections for (n,γ) processes in ^{120}Te , ^{128}Te and ^{130}Te (both for the ground state and first excited state of the daughter nuclides) are given. Some reactions for some isotopes of elements of interest in DBD detectors (Se, Xe, Nd, Cd) or for usual materials of the experimental set-up (Cu, Pb) are also taken into consideration. Nevertheless, as stated for EXFOR, the high quality information compiled in RNAL can be useful to check the reliability of codes developed to study activation in DBD experiments.

3.3 MENDL

MENDL-2 (Medium Energy Nuclear Data Library) [27] contains for 505 stable and unstable target nuclides production cross-sections for the formation of radioactive product nuclides for incident neutrons with energies up to 100 MeV. The nuclides included cover the range from 13-Al-26 to 84-Po-210 with half-lives larger than one day. Cross section for 57500 threshold reactions for the production of product nuclides have been computed with the modified ALICE-92 code. MENDL-2P includes proton cross-sections for 504 nuclei with atomic number from 13 to 84 at energies up to 200 MeV. The data libraries are available from the IAEA Nuclear Data Section being cost-free². Data are given in an ENDF similar format.

The method to obtain cross-sections in MENDL was based on geometry dependent hybrid exciton model [28] and Weisskopf-Ewing model. The multiple precompound nucleon emission was calculated using approach [28] with some corrections. The alpha-particle precompound emission was described in the framework of coalescence pick-up model [29] combined directly with hybrid exciton model. Exciton state density was defined according to the Ericson formula taking into account the Pauli principle and pairing of nuclear levels. To calculate intranuclear transition rate nucleon-nucleon interaction cross-sections corrected for the Pauli principle were used. Level density calculations were performed according to Ignatyuk et al. [30] taking into account the shell effects. The individual level density parameters were used for all nuclei formed in the evaporation cascade. Total

²Available via ftp from <ftp://iaeand.iaea.or.at/>

reaction cross-section and inverse cross-sections were calculated using optical model. Correction of calculated cross-sections was performed for some reaction channels to achieve the agreement with available experimental data. The calculated cross-sections were corrected to reproduce full experimental excitation functions or were normalized to known cross-section values at 14.5 MeV.

MENDL-2 proton cross-sections are calculated on the base of ALICE-IPPE which has some differences with respect to ALICE-91. The algorithm for the level density calculation according to the generalized superfluid model was tested, corrected and improved. The Preequilibrium cluster emission calculation is included in the code. Calculation of the alpha-particle spectra is performed taking into account the pick-up and knock-out processes. The phenomenological approach is used to describe direct channel for the deuteron emission. The triton and ^3He spectra are calculated according to the coalescence pick-up model of Sato, Iwamoto, Harada. The description of the models used may be found in [27]. Corrections were made for cross-sections calculations taking into account gamma-ray emission. The contribution for residual Z-XX-A nucleus production due to photon emission for residual Z-XX-(A-1) or (Z-1)-XX-(A-1) is considered. The corrections were made for the algorithm of multiple pre- compound proton emission spectra calculation near threshold, Kalbach systematic treatment, angular distribution printing algorithm, gamma-spectra printing and for some other instructions.

This library contains very important information for activation in DBD experiments. Cross-sections of isotope production have been compiled for Ge and Te isotopes (for incident neutrons and protons) as well as for many other targets of interest covering a wide range of product nuclides. The main limitation is that the energy range considered is not very large. Just as an example, Tables 7 and 8 in Appendix B show the complete list of produced nuclides considered in MENDL-2 when irradiating with neutrons ^{76}Ge and ^{130}Te (equivalent information for other isotopes can be obtained from <ftp://iaeand.iaea.or.at/>). Unfortunately, no information is given for the production of ^{60}Co in tellurium isotopes due to the large ΔA for the corresponding processes. ^{60}Co is pointed out in [20] to be the main matter of concern for DBD searches due to the cosmogenic activation of TeO_2 crystals.

3.4 Isotope Production Cross Section Libraries for Neutrons and Protons to 1.7 GeV

Experimental, calculated, and evaluated activation libraries for interaction of nucleons with nuclides covering about a third of all natural elements have been produced for validation and development of codes and for modeling isotope production in Refs. [31, 32]. For targets considered, the compilation of experimental data is very complete containing data available on the Web, in journal papers, laboratory reports, theses, and books, as well

as all data included in the large compilation NUCLEX [33]. The evaluated library was produced using all available experimental cross sections together with calculations by the CEM95 (Cascade-Exciton Model), LAHET, and HMS-ALICE (Hybrid Montecarlo Simulation) codes, since neither available experimental data nor any of the current models can be used alone to produce a reliable evaluated activation cross section library covering a large range of target nuclides and incident energies.

Tables 3 and 4 show respectively the 22 end product nuclides (selected because of their medical importance) and the 70 target nuclides of 25 elements taken into consideration in this library. Both proton and neutron irradiation has been studied.

Table 3.— End nuclides whose production cross sections are considered in the library from [31, 32].

^{18}F	^{35}S	^{89}Sr	^{133}Xe
^{22}Na	^{67}Cu	^{89}Zr	^{131}Cs
$^{32}\text{Si} - ^{32}\text{P}$	^{67}Ga	^{95}Zr	^{137}Cs
^{32}P	^{68}Ga	^{95}Nb	^{193m}Pt
^{33}P	$^{68}\text{Ge} - ^{68}\text{Ga}$	^{131}I	^{195m}Pt

The advantages of this library are that it gives results for both neutron and proton induced activation and it is based on experimental measurements and on calculations using the most suitable codes for each target and energy range. The energy coverage (up to 1.7 GeV) is quite good, and although the range of target and product isotopes considered is not very large, it provides very useful (even if not complete) results for germanium. Consequently, this library can be very helpful for germanium DBD experiments. Other targets of interest in the field of DBD like Xe and Mo are also studied.

4 Codes

Since experimental measurements for activation are long, expensive and there are not a great number of available facilities where being carried out, the use of nuclear reaction codes is an appealing solution. In addition, most measurements are performed on targets with the natural composition of isotopes for a given element, often determining only cumulative yields of residual nuclei. Reliable theoretical calculations are required to provide independent yields for isotopically separated targets in many cases.

There are two approaches in the codes used for studies of cosmogenic activation. On one hand, there are codes based on semiempirical formulas for the cross-sections of isotope production and on the other hand, codes based on the complete Monte Carlo (MC) simulation of the hadronic interaction of nucleons with nuclei. The main advantage

Table 4.— Target nuclides for which production cross section are considered in the library from [31, 32].

^{18}O	^{32}S	^{66}Zn	^{89}Y	^{130}Xe	^{193}Ir
	^{33}S	^{67}Zn		^{131}Xe	
^{19}F	^{34}S	^{68}Zn	^{90}Zr	^{132}Xe	^{197}Au
	^{36}S	^{70}Zn	^{91}Zr	^{134}Xe	
^{20}Ne		^{92}Zr		^{136}Xe	^{196}Hg
^{21}Ne	^{35}Cl	^{69}Ga	^{94}Zr		^{198}Hg
^{22}Ne	^{37}Cl	^{71}Ga	^{96}Zr	^{133}Cs	^{199}Hg
					^{200}Hg
^{23}Na	^{36}Ar	^{70}Ge	^{93}Nb	^{134}Ba	^{201}Hg
	^{38}Ar	^{72}Ge		^{135}Ba	^{202}Hg
^{24}Mg	^{40}Ar	^{73}Ge	^{92}Mo	^{136}Ba	^{204}Hg
^{25}Mg		^{74}Ge	^{94}Mo	^{137}Ba	
^{26}Mg	^{39}K	^{76}Ge	^{95}Mo	^{138}Ba	
	^{40}K		^{96}Mo		
	^{41}K		^{97}Mo	^{138}La	
^{27}Al		^{75}As	^{98}Mo	^{139}La	
			^{100}Mo		

of the first approach is that the calculation time is much shorter while Monte Carlo codes are applicable not only to proton-induced but also to neutron-induced nuclear reactions. The relative merits of each approach were examined in detail in [34].

From the first group of codes, the most popular one is COSMO, based of the semiempirical formulas from Silberberg & Tsao [35]. The successive improvements in these formulas have been incorporated in modified versions of the original COSMO [36]. Another code of this type is SIGMA [37], developed at Heidelberg for Ge and Cu targets.

Regarding the MC codes, some general-purpose simulation packages like GEANT4 and FLUKA can be used for activation studies. The main advantage, a priori, of these two codes is that they are continuously evolving and there is a strong support for the users (detailed manuals, web pages, forums, . . .). But there are also a great number of MC codes, or families of codes, specifically devoted to hadronic interactions. Reaction types such as compound nucleus reactions, preequilibrium and direct reactions, spallation, fragmentation and fission have to be considered to study residual nuclei production. The development of most of these codes started in the 1970s and 1980s in very different contexts: studies of cosmic rays and astrophysics, transmutation of nuclear waste or production of medical radioisotopes. Some examples of these codes are: HETC, CEM95,

ISABEL, INUCL, CASCADE, MSDM, ALICE, SHIELD, Many of them are available from the Nuclear Energy Agency (NEA) Data Bank³ and they were compared in a study made at the request of the NEA as part of the programme of work for transmutation of radioactive nuclear waste [38]. The goal of this study was to determine the predictive power of models and codes when calculating activation yields in the energy range up to 5 GeV, evaluating the quality of calculated activation yields for many target elements (O, Al, Fe, Co, Zr, and Au) by comparison with experimental data. They concluded that calculations of activation yields may at best have uncertainties of the order of a factor of two; but frequently, average deviations are much larger (may go up to two or three orders of magnitude). They saw also that there are no general over- or underestimates by individual models or codes, but rather a broad scatter of calculated data. Consequently, it seems very important to choose properly the code to be used for a particular problem. CEM95 and LAHET generally have the best predictive power for spallation reactions at energies above 100 MeV as compared to other codes; at lower energies, the HMS-ALICE code does one of the best jobs. Comparison of the performance of these codes between them and with experimental measurements has been also carried out in other works [39, 40, 41, 42]; a lot of effort has been already devoted to these comparisons, but unfortunately not dealing with activation reactions of interest in DBD experiments.

In this section the main features of COSMO, GEANT4 and FLUKA for studying the problem of activation will be revised. Detailed information for other MC hadronic codes (models used, intercomparison and comparison with experimental data, . . .) can be found in Ref. [38].

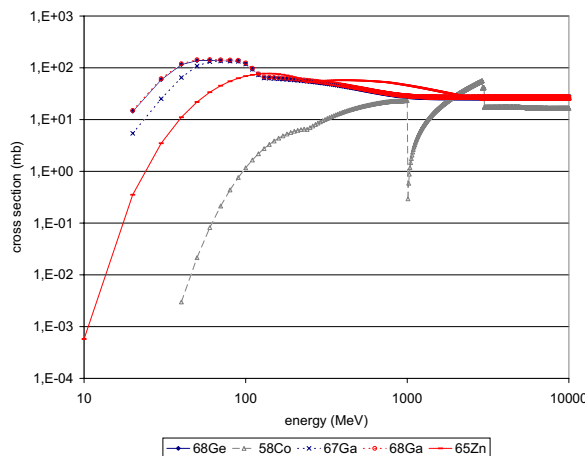


Figure 1.— Excitation functions obtained with COSMO for production of various isotopes from neutron interactions on ^{70}Ge .

³At <http://www.nea.fr/html/dbprog/>

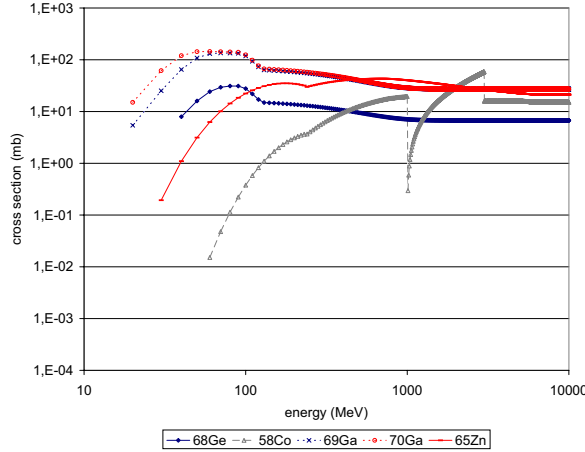


Figure 2.— Excitation functions obtained with COSMO for production of various isotopes from neutron interactions on ^{72}Ge .

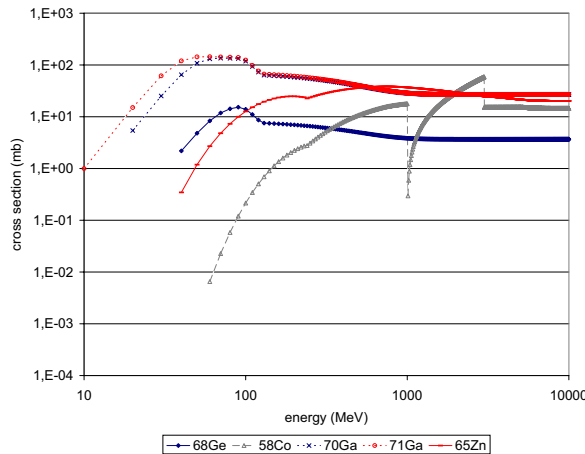


Figure 3.— Excitation functions obtained with COSMO for production of various isotopes from neutron interactions on ^{73}Ge .

4.1 COSMO

Ideally, it would be necessary to know the cross sections for the production of radioactive isotopes from different materials up to the highest energies; unfortunately, only few cross-sections as function of the target mass and energy have been measured for proton and neutron spallation reactions. One solution to this problem has been to collect available experimental data and to build a set of semiempirical formulas.

The Silberberg & Tsao semiempirical formulas [35, 43, 44] give nucleon-nucleus cross sections for different reactions (break-up, spallation, fission, ...) for light and heavy targets, at energies exceeding the 100 MeV. A wide range of product nuclides is taken into account, with very large ΔA between target and product; this is an important feature, since Monte Carlo calculations are very time-consuming when ΔA is large and the energy

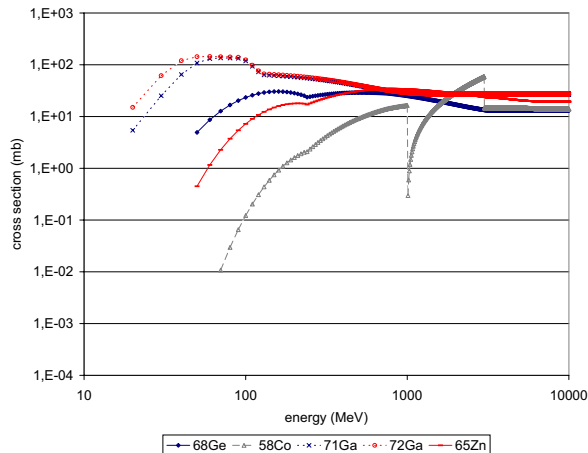


Figure 4.— Excitation functions obtained with COSMO for production of various isotopes from neutron interactions on ^{74}Ge .

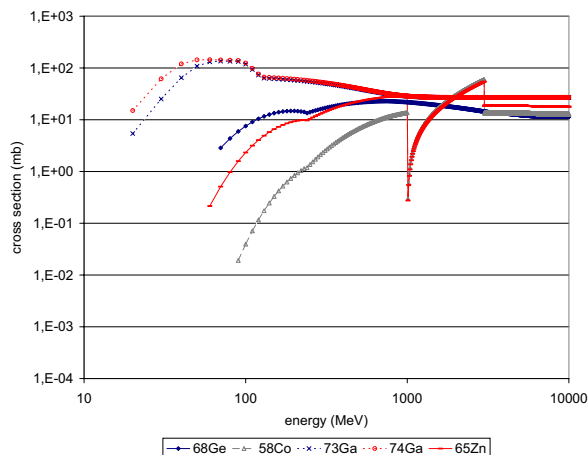


Figure 5.— Excitation functions obtained with COSMO for production of various isotopes from neutron interactions on ^{76}Ge .

is low. These equations improve significantly an earlier attempt to give semiempirical formulas in [45]. For light targets, uncertainties are reported to be from 20 to 30% up to 50 MeV and of 40 % at 2 GeV; for heavy targets, the error is $\sim 50\%$ at 2 GeV [35].

COSMO [36] is a computer program written in FORTRAN coding all necessary computational steps to calculate the nucleon-induced activation yield based of the semiempirical formulas from Silberberg & Tsao [35]. In [46] the code was updated including the new semiempirical formulas from [43] obtained incorporating new cross section measurements; in this version of COSMO also a new set of formulas was included for the tritium production. In this way, the code is able to calculate 275 potentially interesting nuclei and 543 side branch nuclei (with half-lives below one day, being able to decay into a typical cosmogenic impurity). Extensive tests of the code have shown that it underestimates isotope production yields by a factor from two to five for relevant radioactive isotopes [46].

New improvements in the semiempirical formulas have been more recently been released [44]; the addition of these corrections to the code would be highly recommended. The COSMO code allows to get different types of information:

- The production cross section for given target and product isotopes, as a function of the energy.
- The mass yield curve for a given target (summing all nuclides for each mass number).
- The list of all active nuclides produced for given exposure and decaying periods, for a certain material target. The cosmic ray spectrum considered in this calculation has been taken from [47].

The wide range of applicability for targets, products and energies, the fast calculation time and the simplicity of use make COSMO a very useful tool for all kind of activation studies. The still large uncertainties in the results can be partially counterbalanced making estimates also with different codes.

4.2 *GEANT4*

GEANT4 [48] is a toolkit for the simulation of the passage of particles through matter using Object Oriented technology (C++). Its application areas include high energy physics and nuclear experiments, medical, accelerator and space physics studies. GEANT4 provides a complete set of tools for all the domains of detector simulation: Geometry, Tracking, Detector Response, Run, Event and Track management, Visualization and User Interface. An abundant set of Physics Processes handle the diverse interactions of particles with matter across a wide energy range, as required by GEANT4 multi-disciplinary nature; for many physics processes a choice of different models is available. Released the first version in 1999, it is continuously being improved by a world-wide collaboration of about 100 scientists participating in more than 10 experiments in Europe, Russia, Japan, Canada and the United States.

The models implemented in GEANT4 for hadronic interactions are extensively described in [49] and the GEANT4 hadronic physics status is reported in [50]. For modeling final states, three basic types of models are distinguished: models that are predominantly based on experimental or evaluated data, models based on parameterizations and extrapolation of experimental data under some theoretical assumptions, and models based on theory.

A class (called G4NeutronIsotopeProduction) has been implemented to allow the study of isotope production in neutron-induced reactions [51]. This model runs in parasitic model and can be used in conjunction with any set of models for final state production

and inclusive cross sections (the isotope production model complement the transport evaluations in the sense that reaction cross sections and final state information from the transport codes define the interaction rate and particle fluxes, and the isotope production model is used only to predict activation). It is based on evaluated neutron scattering data below neutron kinetic energies up to 20 MeV and a combination of evaluated data and extrapolation at energies up to 100 MeV (including the MENDL-2 data library described in Section 3). Description and results of neutron-induced isotope production model in GEANT4 can be found in [52]. The number of different isotopes the code can handle (targets and products) is very high thanks to the use of the MENDL-2 data; the results are limited by statistics for the very rarely produced isotopes (with very large ΔA between target and product). For other reactions not induced by neutrons, the isotope production is derived from the final state of the transport simulation engines.

Two sets of parameterized models are provided for the simulation of high energy hadron-nucleus interactions. The so-called “low energy model” is intended for hadronic projectiles with incident energies between 1 GeV and 25 GeV, while the “high energy model” is valid for projectiles between 25 GeV and 10 TeV. Both are based on the well-known GHEISHA package of GEANT3. The physics underlying these models comes from an old-fashioned multi-chain model in which the incident particle collides with a nucleon inside the nucleus. The final state of this interaction consists of a recoil nucleon, the scattered incident particle, and possibly many hadronic secondaries. Hadron production is approximated by the formation zone concept, in which the interacting quark-partons require some time and therefore some range to hadronize into real particles. All of these particles are able to re-interact within the nucleus, thus developing an intra-nuclear cascade. In these models only the first hadron-nucleon collision is simulated in detail. The remaining interactions within the nucleus are simulated by generating additional hadrons and treating them as secondaries from the initial collision. The numbers, types and distributions of the extra hadrons are determined by functions which were fitted to experimental data or which reproduce general trends in hadron-nucleus collisions. Numerous tunable parameters are used throughout these models to obtain reasonable physical behavior. This restricts the use of these models as generators for hadron-nucleus interactions because it is not always clear how the parameters relate to physical quantities.

Theory based modeling is the basic approach in many models that are provided by or in development for GEANT4. It includes a set of different theoretical approaches to describe hadronic interactions, depending on the addressed energy range and CPU constraints. Parton string models for the simulation of high energy final states (above 5 GeV) are provided and in further development [53]. Below 5 GeV, intra-nuclear transport models are provided [54]. For cascade type models a rewrite of HETC and INUCL is provided, as well as an implementation of a time-like cascade. At energies below 100

MeV the possibility of using exciton based pre-compound models is offered. The last phase of a nuclear interaction is nuclear evaporation. To model the behaviour of excited, thermalized nuclei, variants of the classical Weisskopf-Ewing model are used. Specialized improvements such as Fermi's break-up model for light nuclei and multi-fragmentation for very high excitation energies are employed. Fission and photon evaporation can be treated as competitive channels in the evaporation model.

Therefore, GEANT4 is a valuable instrument to perform activation studies for a wide range of targets, products, projectiles and energies. Uncertainties in the results will depend on the particular models implemented by the users in their applications.

4.3 FLUKA

FLUKA [55] is a fully integrated particle physics MonteCarlo simulation package written in FORTRAN. It has many applications in high energy experimental physics and engineering, shielding, detector and telescope design, cosmic ray studies, dosimetry, medical physics and radio-biology. FLUKA is capable of handling transport and interactions of hadronic and electromagnetic particles in any material over a wide energy range, from thermal neutrons to cosmic rays. It is intrinsically an analog code but can be run in biased mode for a variety of deep penetration applications. Interactions are treated in a theory-driven approach, and models and model implementations are always guided and checked against experimental data. Hadron-nucleon interaction models are based on resonance production and decay below a few GeV, and on the Dual Parton Model (DPM). Two models are also used in hadron-nucleus interactions. At momenta below 3-5 GeV/c the so-called PEANUT includes a very detailed Generalized IntraNuclear Cascade (GING) and a preequilibrium stage, while at high energies the Gribov-Glauber multiple collision mechanism is included in a less refined GINC. Both modules are followed by equilibrium processes: evaporation, fission, Fermi break-up, γ deexcitation. A specialized multigroup transport, based on a dedicated neutron library, is implemented for low energy (≤ 20 MeV) neutrons. A description of the intermediate and high energy hadronic interaction models used in FLUKA can be found in Ref. [56].

In principle, FLUKA can be used without writing code, just creating an input file with a series of input cards which define the properties of the primary particles (type, energy/momentum, position and direction), the geometry (dimensions and materials), the physical processes to be taken into account and the information to be recorded during the simulation. FLUKA offers different options (called "estimators") to save this information; for activation studies the estimator of interest is RESNUCLEI, which scores residual nuclei produced on a selected region. All residual nuclei are scored when they have been fully de-excited down to their ground or isomeric state. The scoring does not distinguish between

ground state and isomeric state (they are scored as the same isotope) and radioactive decay is not performed by FLUKA.

Isotope production induced by both neutrons and protons can be simulated with FLUKA in a large energy interval, providing a wide range of ΔA for the daughter nuclides. The main limitation of FLUKA is the limited availability of data for the target materials in activation studies. Table 9 in Appendix C shows the list of materials for which neutron cross-sections are available in the version 2003.1 of FLUKA; the fourth column of Table 9 indicates if there are information for residual nuclei production. No neutron data is available for tellurium, and for germanium there are not information for nuclei production. Consequently, at present FLUKA cannot be used for activation studies in the detector materials with the greatest interest in DBD. However it could be used for other materials like copper or lead.

5 Results for activation in Germanium

Germanium detectors have produced up to now the most relevant results for neutrinoless DBD and the effective neutrino mass (see a compilation of results in [6]) thanks to their extremely good energy resolution and radiopurity, good efficiency and the enrichment in the DBD emitter ^{76}Ge . As shown in Table 1, many of the new DBD projects are still based on germanium. Consequently, this material has been chosen here as an example to illustrate the problem of cosmogenic activation. In this section results for some relevant production cross sections in isotopes of natural germanium will be collected and compared. Cross section data have been obtained from different sources presented in the previous sections including data libraries, MC codes and semiempirical formulas:

- In Ref. [18], theoretical and experimental investigation of cosmogenic radioisotope production in Germanium was made. Neutron-induced excitation functions, $\sigma(E)$, were calculated using a spallation reaction code extension of a compound nucleus reaction code for ^{70}Ge , ^{72}Ge , ^{73}Ge , ^{74}Ge and ^{76}Ge as targets and ^{68}Ge , ^{65}Zn , ^{58}Co , ^{A-2}Ga and ^{A-3}Ga as products. Figures 2-6 in [18] show the results.
- The same excitation functions have been calculated in this work using the modified version of the COSMO code from [46] and are plotted in Figs. 1- 5.
- These cross sections have been also plotted using the data from the MENDL-2 library in Figs. 6- 10. In this case only energies up to 100 MeV are available.
- Some of these cross sections have been also estimated using the MC codes CEM95 and HMS-ALICE in [32]. Pages A25-A30 of Appendix A in [32] show results for the production of ^{68}Ge in the five isotopes of natural germanium as well as the production of ^{67}Ga and ^{68}Ga in ^{70}Ge .

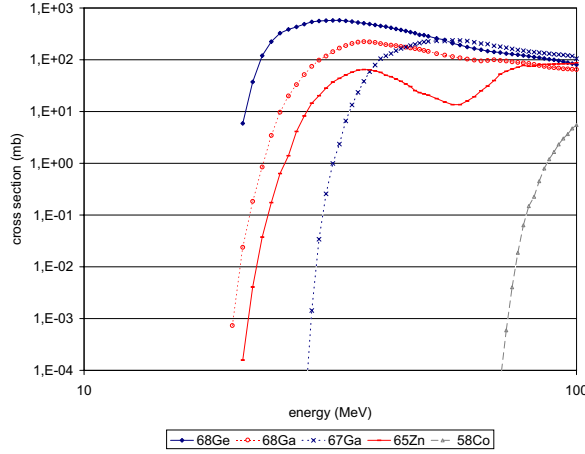


Figure 6.— Excitation functions from MENDL [27] for production of various isotopes from neutron interactions on ^{70}Ge .

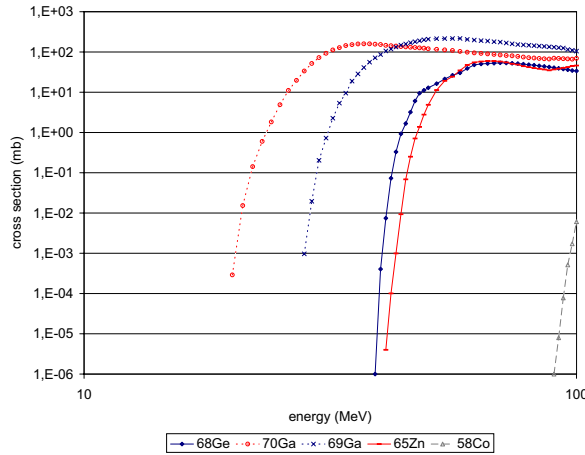


Figure 7.— Excitation functions from MENDL [27] for production of various isotopes from neutron interactions on ^{72}Ge .

Comparing these four sources of information on isotope production in natural germanium, significant differences in the values and shapes of the excitation functions are found. There is no better agreement neither for any particular pair of sources nor for certain energy ranges or nuclides.

The couple of isotopes ^{68}Ge and his daughter ^{68}Ga represent a serious potential background due to the long half-life of the parent (270.82 days) and the decay energy of the daughter ($Q_{\beta^+}=2921.1$ keV), which makes them contribute to the energy region where the signal of neutrinoless DBD of ^{76}Ge is expected to appear (a peak around 2039 keV). An extensive discussion of the effects of cosmogenic induced isotopes in germanium detectors can be found in [19]. The problem of the cosmogenic production of ^{68}Ge is specially acute because all non-germanium isotopes (like ^{60}Co) induced in the germanium material can

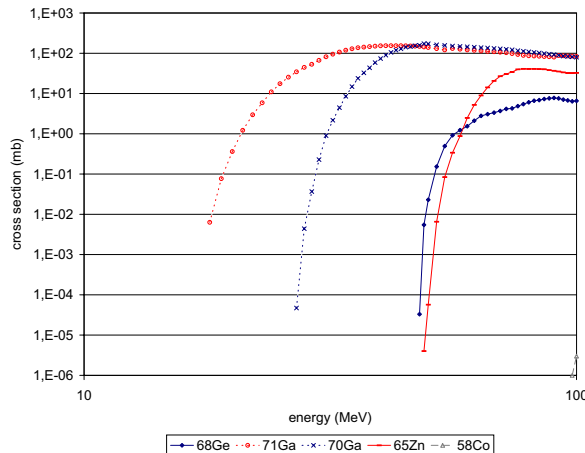


Figure 8.— Excitation functions from MENDL [27] for production of various isotopes from neutron interactions on ^{73}Ge .

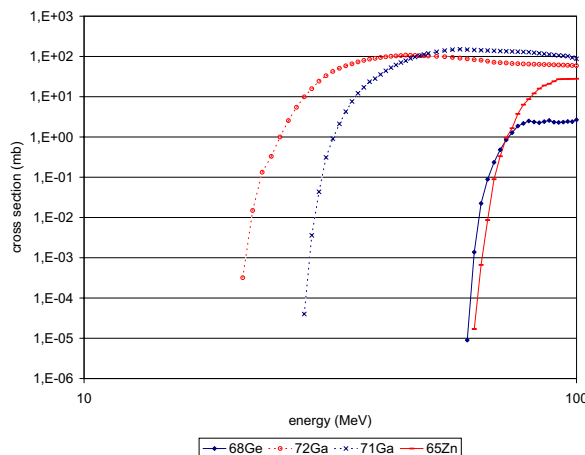


Figure 9.— Excitation functions from MENDL [27] for production of various isotopes from neutron interactions on ^{74}Ge .

be removed by zone melting. Table 5 shows a comparison of the cross-sections for ^{68}Ge production in ^{76}Ge at different energies from all the available sources; results differ up to by a factor ~ 50 .

Since neutron induced activation measurements are even more scarce than those using proton beams, isotope production cross sections for neutrons and protons like projectiles are usually considered to be equal. Data from Refs. [27] and [32], which give information for both neutron and proton induced activation, have been compared in order to assess the above mentioned assumption for the cases of interest in DBD.

According to plots shown in [32], differences are not negligible in the excitation functions for neutrons and protons calculated in natural germanium isotopes; differences reach up to one order of magnitude in the cross section values. Shapes and thresholds are also different in some cases. No clear trend can be identified for the kind of projectile or en-

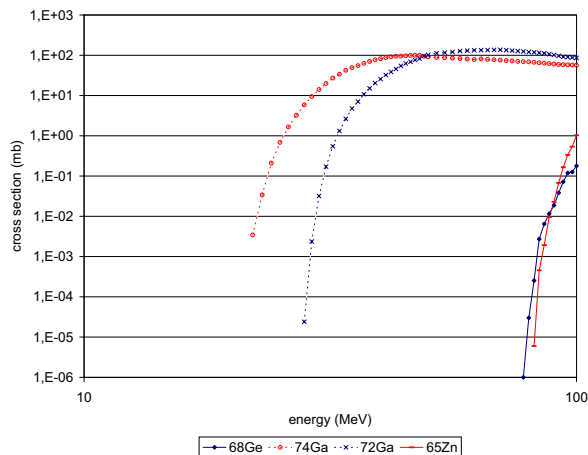


Figure 10.— Excitation functions from MENDL [27] for production of various isotopes from neutron interactions on ^{76}Ge .

Table 5.— Comparison of different estimates of the production cross section (in mb) of ^{68}Ge in ^{76}Ge by neutrons with 100, 1000 or 10000 MeV.

Energy (MeV)	Ref. [46]	Ref. [27]	Ref. [18]	Ref. [32]
100	7.5	0.2	0.7	6
1000	22		10	0.4
10000	11			

ergy range. However, for the production of the most dangerous isotope due to cosmogenic activation in germanium detectors, ^{68}Ge , excitation functions from [32] are very similar for neutrons and protons in all natural germanium isotopes except for ^{76}Ge , for which proton induced activation is slightly higher than the neutron induced one. Figures 11-15 compare for all the isotopes in natural germanium the cross sections for production of ^{68}Ge induced by neutrons or by protons, according to the MENDL library [27]. Equivalent plots can be obtained for the production of other isotopes in germanium or other target materials using MENDL data.

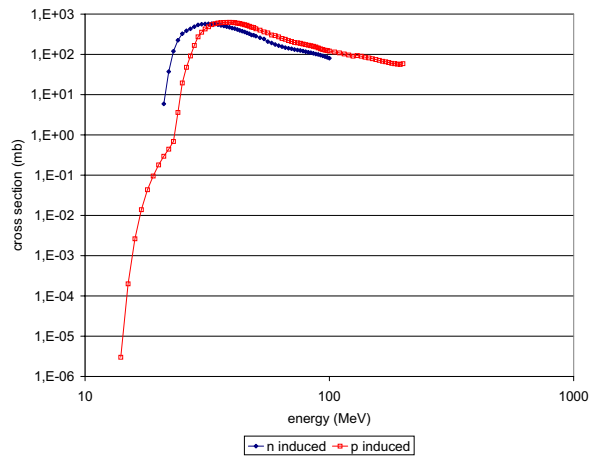


Figure 11.— Comparison of the cross sections for production of ^{68}Ge on ^{70}Ge induced by neutrons or by protons, according to the MENDL library [27].

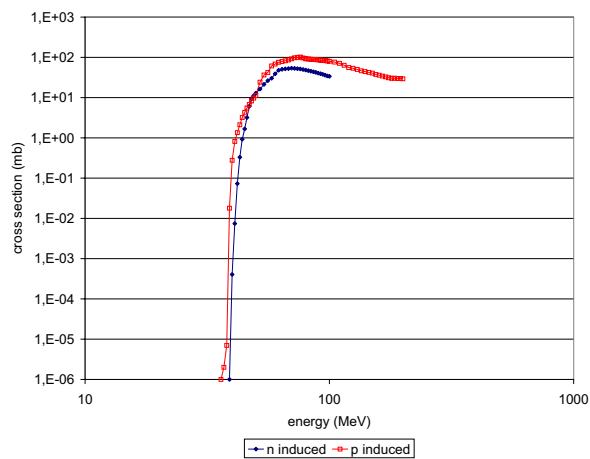


Figure 12.— Comparison of the cross sections for production of ^{68}Ge on ^{72}Ge induced by neutrons or by protons, according to the MENDL library [27].

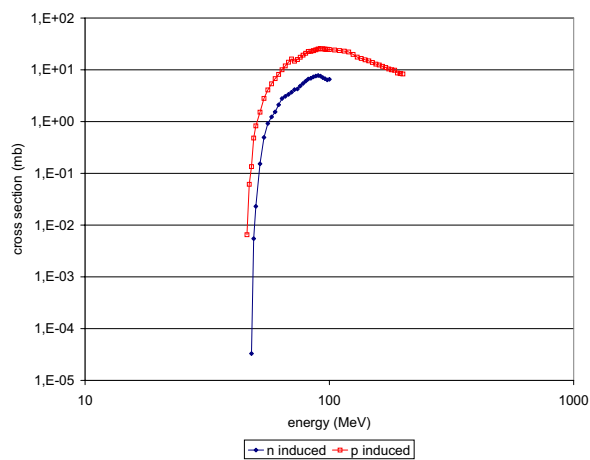


Figure 13.— Comparison of the cross sections for production of ^{68}Ge on ^{73}Ge induced by neutrons or by protons, according to the MENDL library [27].

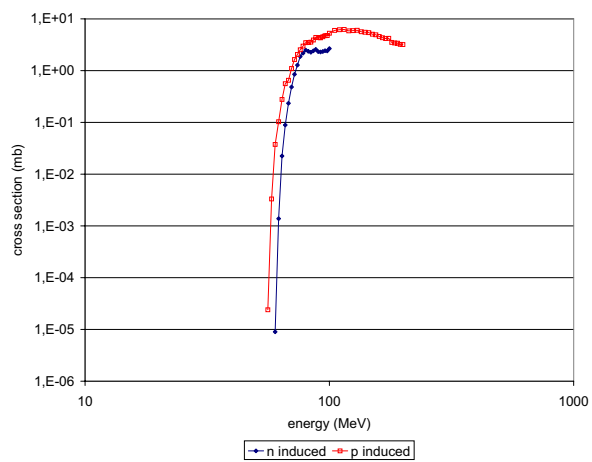


Figure 14.— Comparison of the cross sections for production of ^{68}Ge on ^{74}Ge induced by neutrons or by protons, according to the MENDL library [27].

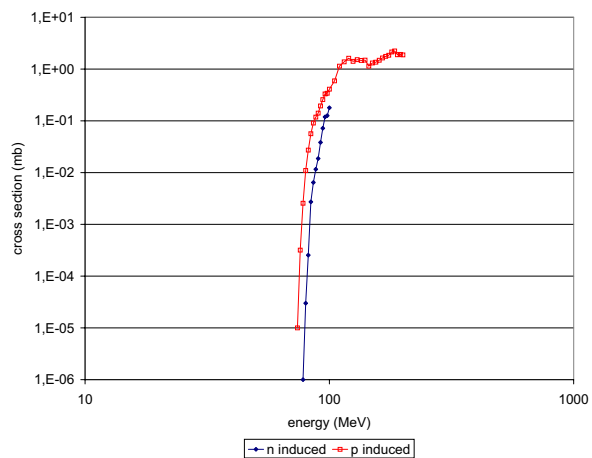


Figure 15.— Comparison of the cross sections for production of ^{68}Ge on ^{76}Ge induced by neutrons or by protons, according to the MENDL library [27].

6 Conclusions

An overview of nuclear data libraries and computational codes which can be used in studies of cosmogenic activation of materials in DBD experiments has been made.

Four different data libraries have been examined searching for isotope production cross sections of interest in DBD experiments. MENDL gives a very complete information: for all isotopes of natural germanium and tellurium (as well as for many other elements) it covers a very wide range of product nuclides, either for neutrons or protons as projectiles. Consequently, MENDL can be a priceless tool in activation studies. The only drawback is the limited range of energies taken into consideration (100 MeV for neutrons, 200 MeV for protons). The library from [31, 32] can be also very helpful, specially for germanium DBD experiments, since it is based both on measurements and selected calculations in a wide energy range. The other two libraries, RNAL and EXFOR, provide data on a very limited number of activation reactions with low interest in DBD experiments; nevertheless, these data can be useful to check and evaluate the reliability of codes developed to determine production cross sections relevant in the field of DBD.

Two different kind of computational codes can be used in activation studies. COSMO follows the approach of using semiempirical formulas to estimate the isotope production cross sections. It can be applied for a wide range of targets, products and energies including those of interest for activation in DBD experiments. The fast calculation time and the simplicity of use make COSMO a very useful tool for all kind of activation studies. Uncertainties of a factor of two have been reported using this code. The other approach is using Monte Carlo codes to simulate nuclear reactions. Many of this type of codes were carefully analyzed in Ref. [38], concluding that prediction of activation yields has at best an uncertainty of a factor two. Here, the potential of other two MC codes has been studied. It has been concluded that FLUKA cannot be used at present for determining activation in materials of crucial interest in DBD like germanium and tellurium. GEANT4, which uses data from the MENDL-2 library for neutron-induced isotope production, can be applied for activation studies for a wide range of targets, products, projectiles and energies, depending the uncertainties in the results on the particular models implemented by the users.

Results for the isotope production cross sections in germanium, the preferred detector material in present and future DBD projects, have been compared using data from different sources: libraries, Monte Carlo calculations and semiempirical formulas. Significant differences in shapes and values of excitation functions have been found, with no clear trend neither for isotopes nor for energy range. For the production of ^{68}Ge in ^{76}Ge (the most relevant pair of product-target in enriched germanium detectors) differences from the several estimates reach up to a factor ~ 50 .

As it can be deduced from the particular results shown in Section 5 and from the general conclusions drawn in this and in other studies of the problem of activation, the precision of present estimates of production cross sections based on Monte Carlo or on semiempirical formulas is not enough for having accurate calculations of the isotope production yield due to exposure to cosmic rays in DBD experiments when materials are above ground. Experimental measurements on isotope production cross sections and further development on models and codes are still necessary to obtain precisely quantitative information.

Appendix A

Table 6: List of targets and reactions whose cross sections are included in the RNAL library (taken from [26]).

1	H-1	(n,g)	2	B-10	(n,a)
3	C-12	(n,2n)	4	C-12	(n,g)
5	C-13	(n,g)	6	N-14	(n,p)
7	O-16	(n,na)	8	O-16	(n,p)
9	F-19	(n,2n)	10	Na-23	(n,2n)
11	Na-23	(n,g)	12	Mg-24	(n,p)
13	Mg-26	(n,g)	14	Al-27	(n,2n)
15	Al-27	(n,na)	16	Al-27	(n,g)
17	Al-27	(n,p)	18	Al-27	(n,a)
19	Si-28	(n,p)	20	Si-28	(n,np)
20	Si-28	(n,d)	21	Si-29	(n,p)
22	Si-29	(n,np)	22	Si-29	(n,d)
23	Si-29	(n,t)	24	Si-30	(n,a)
25	Si-30	(n,g)	26	P-31	(n,g)
27	P-31	(n,p)	28	P-31	(n,a)
29	S-32	(n,p)	30	S-34	(n,g)
31	S-34	(n,p)	32	S-36	(n,g)
33	Cl-35	(n,2n)	34	Cl-35	(n,g)
35	Cl-37	(n,g)	36	Cl-37	(n,p)
37	Cl-37	(n,a)	38	Ar-36	(n,g)
39	Ar-38	(n,g)	40	Ar-40	(n,g)
41	K-39	(n,p)	42	K-41	(n,g)
43	K-41	(n,a)	44	Ca-40	(n,g)
45	Ca-44	(n,p)	46	Ca-45	(n,a)
47	Ca-48	(n,g)	48	Sc-45	(n,g)
49	Ti-46	(n,2n)	50	Ti-46	(n,p)
51	Ti-47	(n,p)	52	Ti-47	(n,np+d)
53	Ti-48	(n,p)	54	Ti-48	(n,np)
54	Ti-48	(n,d)	55	Ti-48	(n,a)
56	Ti-50	(n,a)	57	Ti-50	(n,g)
58	V-50	(n,2n)	59	V-51	(n,g)
60	V-51	(n,p)	61	V-51	(n,a)
62	Cr-50	(n,g)	63	Cr-52	(n,2n)

64	Cr-52	(n,p)	65	Cr-53	(n,np)
65	Cr-53	(n,d)	66	Cr-54	(n,g)
67	Cr-54	(n,a)	68	Mn-53	(n,g)
69	Mn-55	(n,2n)	70	Mn-55	(n,g)
71	Mn-55	(n,a)	72	Fe-54	(n,2n)
73	Fe-54	(n,g)	74	Fe-54	(n,p)
75	Fe-56	(n,2n)	76	Fe-56	(n,g)
77	Fe-56	(n,p)	78	Fe-57	(n,g)
79	Fe-58	(n,g)	80	Fe-60	(n,g)
81	Co-59	(n,2n)	82	Co-59	(n,g)
83	Co-59	(n,a)	84	Co-60	(n,g)
85	Co-60	(n,p)	86	Ni-58	(n,2n)
87	Ni-58	(n,g)	88	Ni-58	(n,p)
89	Ni-58	(n,np)	90	Ni-60	(n,2n)
91	Ni-60	(n,p)	92	Ni-61	(n,g)
93	Ni-62	(n,g)	94	Ni-64	(n,2n)
95	Ni-64	(n,g)	96	Cu-63	(n,2n)
97	Cu-63	(n,g)	98	Cu-63	(n,p)
99	Cu-63	(n,a)	100	Cu-65	(n,2n)
101	Cu-65	(n,g)	102	Zn-64	(n,g)
103	Zn-64	(n,p)	104	Zn-66	(n,p)
105	Zn-68	(n,g)	106	Zn-70	(n,g)
107	Ga-69	(n,g)	108	Ga-69	(n,a)
109	Ga-71	(n,g)	110	Se-74	(n,g)
111	Se-78	(n,g)	112	Se-79	(n,g)
113	Se-80	(n,g)	114	Se-82	(n,g)
115	Kr-80	(n,g)	116	Kr-84	(n,g)
117	Kr-86	(n,g)	118	Rb-85	(n,g)
119	Sr-84	(n,g)	120	Sr-89	(n,g)
121	Sr-90	(n,g)	122	Zr-90	(n,2n)
123	Zr-93	(n,g)	124	Zr-94	(n,g)
125	Zr-96	(n,2n)	126	Nb-93	(n,n')
127	Nb-93	(n,2n)	128	Nb-93	(n,g)
129	Mo-92	(n,g)	130	Mo-92	(n,p)
131	Mo-92	(n,d+np)	132	Mo-93	(n,np)
132	Mo-93	(n,d)	133	Mo-94	(n,2n)
134	Mo-94	(n,p)	135	Mo-94	(n,np)
135	Mo-94	(n,d)	136	Mo-95	(n,p)

137	Mo-95	(n,np)	137	Mo-95	(n,d)
138	Mo-98	(n,g)	139	Mo-100	(n,2n)
140	Mo-100	(n,g)	141	Tc-99	(n,2n)
142	Ru-96	(n,g)	143	Ru-102	(n,g)
144	Ru-104	(n,g)	145	Rh-103	(n,n')
146	Rh-103	(n,g)	147	Pd-102	(n,g)
148	Pd-108	(n,g)	149	Pd-110	(n,g)
150	Ag-107	(n,g)	151	Ag-108m	(n,g)
152	Ag-109	(n,2n)	153	Ag-109	(n,g)
154	Cd-106	(n,g)	155	Cd-108	(n,g)
156	Cd-114	(n,g)	157	In-113	(n,g)
158	In-115	(n,n')	159	In-115	(n,g)
160	Sn-120	(n,g)	161	Sn-121	(n,g)
162	Sn-122	(n,2n)	163	Sn-125	(n,g)
164	Sn-126	(n,g)	165	Sb-123	(n,g)
166	Sb-124	(n,g)	167	Te-120	(n,g)
168	Te-128	(n,g)	169	Te-130	(n,g)
170	I-127	(n,2n)	171	I-127	(n,g)
172	I-128	(n,g)	173	Xe-134	(n,g)
174	Xe-136	(n,g)	175	Cs-133	(n,g)
176	Cs-135	(n,g)	177	Cs-136	(n,g)
178	Cs-137	(n,g)	179	Ba-130	(n,g)
180	Ba-132	(n,g)	181	Ba-137	(n,p)
182	Ba-138	(n,a)	183	La-138	(n,g)
184	La-139	(n,g)	185	Ce-143	(n,g)
186	Nd-146	(n,g)	187	Nd-148	(n,g)
188	Nd-150	(n,g)	189	Sm-144	(n,g)
190	Sm-152	(n,g)	191	Sm-154	(n,g)
192	Eu-151	(n,2n)	193	Eu-151	(n,g)
194	Eu-153	(n,2n)	195	Eu-153	(n,g)
196	Eu-154	(n,g)	197	Tb-159	(n,2n)
198	Tb-159	(n,g)	199	Dy-158	(n,g)
200	Dy-158	(n,p)	201	Dy-164	(n,g)
202	Ho-165	(n,g)	203	Er-162	(n,g)
204	Er-164	(n,g)	205	Er-168	(n,g)
206	Er-170	(n,g)	207	Tm-169	(n,g)
208	Yb-168	(n,g)	209	Yb-174	(n,g)
210	Yb-176	(n,g)	211	Lu-175	(n,g)

212	Lu-176	(n,g)	213	Hf-174	(n,g)
214	Hf-179	(n,2n)	215	Ta-181	(n,3n)
216	Ta-181	(n,g)	217	W-182	(n,2n)
218	W-182	(n,na)	219	W-183	(n,g)
220	W-184	(n,g)	221	W-186	(n,2n)
222	W-186	(n,na)	223	W-186	(n,g)
224	Re-185	(n,2n)	225	Re-185	(n,g)
226	Re-187	(n,2n)	227	Re-187	(n,g)
228	Re-187	(n,p)	229	Os-184	(n,g)
230	Os-188	(n,g)	231	Os-190	(n,g)
232	Os-190	(n,a)	233	Os-192	(n,g)
234	Ir-191	(n,g)	235	Ir-192n	(n,n')
236	Ir-192	(n,g)	237	Ir-193	(n,2n)
238	Pt-190	(n,g)	239	Pt-192	(n,g)
240	Pt-194	(n,g)	241	Pt-196	(n,g)
242	Pt-198	(n,g)	243	Au-197	(n,2n)
244	Au-197	(n,g)	245	Hg-196	(n,g)
246	Hg-202	(n,g)	247	Hg-204	(n,g)
248	Tl-203	(n,g)	249	Tl-205	(n,g)
250	Pb-204	(n,2n)	251	Pb-206	(n,2n)
252	Pb-206	(n,a)	253	Pb-208	(n,g)
254	Bi-209	(n,2n)	255	Bi-209	(n,g)

Appendix B

Table 7: List of isotopes whose production cross sections are included in the MENDL-2 library for ^{76}Ge as target and neutrons as projectile. The reactions which give rise to each nuclide are also indicated.

(n,2n)	GE 75	(n,3n)	GE 74
(n,4n)	GE 73	(n,p)	GA 76
(n,2p)	ZN 75	(n,5n)	GE 72
(n,6n)	GE 71	(n,7n)	GE 70
(n,8n)	GE 69	(n,9n)	GE 68
(n,10n)	GE 67	(n,11n)	GE 66
(n,np)+(n,d)	GA 75	(n,2np)+(n,nd)	GA 74
(n,3np)+(n,2nd)	GA 73	(n,4np)+(n,3nd)	GA 72
(n,5np)+(n,4nd)	GA 71	(n,6np)+(n,5nd)	GA 70
(n,7np)+(n,6nd)	GA 69	(n,8np)+(n,7nd)	GA 68
(n,9np)+(n,8nd)	GA 67	(n,10np)+(n,9nd)	GA 66
(n,n2p)+(n,1pd)	ZN 74	(n,2n2p)+(n,X)	ZN 73
(n,3n2p)+(n,X)	ZN 72	(n,4n2p)+(n,X)	ZN 71
(n,5n2p)+(n,X)	ZN 70	(n,6n2p)+(n,X)	ZN 69
(n,7n2p)+(n,X)	ZN 68	(n,8n2p)+(n,X)	ZN 67
(n,9n2p)+(n,X)	ZN 66	(n,10n2p)+(n,X)	ZN 65
(n,11n2p)+(n,X)	ZN 64	(n,12n2p)+(n,X)	ZN 63
(n,3p)	CU 74	(n,n3p)+(n,2pd)	CU 73
(n,2n3p)+(n,X)	CU 72	(n,3n3p)+(n,X)	CU 71
(n,4n3p)+(n,X)	CU 70	(n,5n3p)+(n,X)	CU 69
(n,6n3p)+(n,X)	CU 68	(n,7n3p)+(n,X)	CU 67
(n,8n3p)+(n,X)	CU 66	(n,9n3p)+(n,X)	CU 65
(n,10n3p)+(n,X)	CU 64	(n,11n3p)+(n,X)	CU 63
(n,12n3p)+(n,X)	CU 62	(n,4p)	NI 73
(n,n4p)+(n,3pd)	NI 72	(n,2n4p)+(n,X)	NI 71
(n,3n4p)+(n,X)	NI 70	(n,4n4p)+(n,X)	NI 69
(n,5n4p)+(n,X)	NI 68	(n,6n4p)+(n,X)	NI 67
(n,7n4p)+(n,X)	NI 66	(n,8n4p)+(n,X)	NI 65
(n,9n4p)+(n,X)	NI 64	(n,10n4p)+(n,X)	NI 63
(n,11n4p)+(n,X)	NI 62	(n,12n4p)+(n,X)	NI 61
(n,13n4p)+(n,X)	NI 60	(n,5p)	CO 72

$(n, n5p) + (n, 4pd)$	CO 71	$(n, 2n5p) + (n, X)$	CO 70
$(n, 3n5p) + (n, X)$	CO 69	$(n, 4n5p) + (n, X)$	CO 68
$(n, 5n5p) + (n, X)$	CO 67	$(n, 6n5p) + (n, X)$	CO 66
$(n, 7n5p) + (n, X)$	CO 65	$(n, 8n5p) + (n, X)$	CO 64
$(n, 9n5p) + (n, X)$	CO 63	$(n, 10n5p) + (n, X)$	CO 62
$(n, 11n5p) + (n, X)$	CO 61	$(n, 12n5p) + (n, X)$	CO 60
$(n, 13n5p) + (n, X)$	CO 59	$(n, 6p)$	FE 71
$(n, n6p) + (n, 5pd)$	FE 70	$(n, 2n6p) + (n, X)$	FE 69
$(n, 3n6p) + (n, X)$	FE 68	$(n, 4n6p) + (n, X)$	FE 67
$(n, 5n6p) + (n, X)$	FE 66	$(n, 6n6p) + (n, X)$	FE 65
$(n, 7n6p) + (n, X)$	FE 64	$(n, 8n6p) + (n, X)$	FE 63
$(n, 9n6p) + (n, X)$	FE 62	$(n, 10n6p) + (n, X)$	FE 61
$(n, 11n6p) + (n, X)$	FE 60	$(n, 12n6p) + (n, X)$	FE 59
$(n, 13n6p) + (n, X)$	FE 58	$(n, 14n6p) + (n, X)$	FE 57
$(n, 2n7p) + (n, X)$	MN 68	$(n, 3n7p) + (n, X)$	MN 67
$(n, 4n7p) + (n, X)$	MN 66	$(n, 5n7p) + (n, X)$	MN 65
$(n, 6n7p) + (n, X)$	MN 64	$(n, 7n7p) + (n, X)$	MN 63
$(n, 8n7p) + (n, X)$	MN 62	$(n, 9n7p) + (n, X)$	MN 61
$(n, 10n7p) + (n, X)$	MN 60	$(n, 11n7p) + (n, X)$	MN 59
$(n, 12n7p) + (n, X)$	MN 58	$(n, 13n7p) + (n, X)$	MN 57
$(n, 4n8p) + (n, X)$	CR 65	$(n, 5n8p) + (n, X)$	CR 64
$(n, 6n8p) + (n, X)$	CR 63	$(n, 7n8p) + (n, X)$	CR 62
$(n, 8n8p) + (n, X)$	CR 61	$(n, 9n8p) + (n, X)$	CR 60
$(n, 10n8p) + (n, X)$	CR 59	$(n, 11n8p) + (n, X)$	CR 58
$(n, 12n8p) + (n, X)$	CR 57	$(n, 13n8p) + (n, X)$	CR 56
$(n, 14n8p) + (n, X)$	CR 55	$(n, 15n8p) + (n, X)$	CR 54

Table 8: List of isotopes whose production cross sections are included in the MENDL-2 library for ^{130}Te as target and neutrons as projectile. The reactions which give rise to each nuclide are also indicated.

(n,2n)	TE129	(n,3n)	TE128
(n,4n)	TE127	(n,p)	SB130
(n,2p)	SN129	(n,5n)	TE126
(n,6n)	TE125	(n,7n)	TE124
(n,8n)	TE123	(n,9n)	TE122
(n,10n)	TE121	(n,11n)	TE120
(n,12n)	TE119	(n,np)+(n,d)	SB129
(n,2np)+(n,nd)	SB128	(n,3np)+(n,2nd)	SB127
(n,4np)+(n,3nd)	SB126	(n,5np)+(n,4nd)	SB125
(n,6np)+(n,5nd)	SB124	(n,7np)+(n,6nd)	SB123
(n,8np)+(n,7nd)	SB122	(n,9np)+(n,8nd)	SB121
(n,10np)+(n,9nd)	SB120	(n,11np)+(n,10nd)	SB119
(n,12np)+(n,11nd)	SB118	(n,n2p)+(n,1pd)	SN128
(n,2n2p)+(n,X)	SN127	(n,3n2p)+(n,X)	SN126
(n,4n2p)+(n,X)	SN125	(n,5n2p)+(n,X)	SN124
(n,6n2p)+(n,X)	SN123	(n,7n2p)+(n,X)	SN122
(n,8n2p)+(n,X)	SN121	(n,9n2p)+(n,X)	SN120
(n,10n2p)+(n,X)	SN119	(n,11n2p)+(n,X)	SN118
(n,12n2p)+(n,X)	SN117	(n,13n2p)+(n,X)	SN116
(n,3p)	IN128	(n,n3p)+(n,2pd)	IN127
(n,2n3p)+(n,X)	IN126	(n,3n3p)+(n,X)	IN125
(n,4n3p)+(n,X)	IN124	(n,5n3p)+(n,X)	IN123
(n,6n3p)+(n,X)	IN122	(n,7n3p)+(n,X)	IN121
(n,8n3p)+(n,X)	IN120	(n,9n3p)+(n,X)	IN119
(n,10n3p)+(n,X)	IN118	(n,11n3p)+(n,X)	IN117
(n,12n3p)+(n,X)	IN116	(n,4p)	CD127
(n,n4p)+(n,3pd)	CD126	(n,2n4p)+(n,X)	CD125
(n,3n4p)+(n,X)	CD124	(n,4n4p)+(n,X)	CD123
(n,5n4p)+(n,X)	CD122	(n,6n4p)+(n,X)	CD121
(n,7n4p)+(n,X)	CD120	(n,8n4p)+(n,X)	CD119
(n,9n4p)+(n,X)	CD118	(n,10n4p)+(n,X)	CD117
(n,11n4p)+(n,X)	CD116	(n,12n4p)+(n,X)	CD115
(n,13n4p)+(n,X)	CD114	(n,14n4p)+(n,X)	CD113

(n,5p)	AG126	(n,n5p)+(n,4pd)	AG125
(n,2n5p)+(n,X)	AG124	(n,3n5p)+(n,X)	AG123
(n,4n5p)+(n,X)	AG122	(n,5n5p)+(n,X)	AG121
(n,6n5p)+(n,X)	AG120	(n,7n5p)+(n,X)	AG119
(n,8n5p)+(n,X)	AG118	(n,9n5p)+(n,X)	AG117
(n,10n5p)+(n,X)	AG116	(n,11n5p)+(n,X)	AG115
(n,12n5p)+(n,X)	AG114	(n,13n5p)+(n,X)	AG113
(n,6p)	PD125	(n,n6p)+(n,5pd)	PD124
(n,2n6p)+(n,X)	PD123	(n,3n6p)+(n,X)	PD122
(n,4n6p)+(n,X)	PD121	(n,5n6p)+(n,X)	PD120
(n,6n6p)+(n,X)	PD119	(n,7n6p)+(n,X)	PD118
(n,8n6p)+(n,X)	PD117	(n,9n6p)+(n,X)	PD116
(n,10n6p)+(n,X)	PD115	(n,11n6p)+(n,X)	PD114
(n,12n6p)+(n,X)	PD113	(n,13n6p)+(n,X)	PD112
(n,14n6p)+(n,X)	PD111	(n,15n6p)+(n,X)	PD110
(n,2n7p)+(n,X)	RH122	(n,3n7p)+(n,X)	RH121
(n,4n7p)+(n,X)	RH120	(n,5n7p)+(n,X)	RH119
(n,6n7p)+(n,X)	RH118	(n,7n7p)+(n,X)	RH117
(n,8n7p)+(n,X)	RH116	(n,9n7p)+(n,X)	RH115
(n,10n7p)+(n,X)	RH114	(n,11n7p)+(n,X)	RH113
(n,12n7p)+(n,X)	RH112	(n,13n7p)+(n,X)	RH111
(n,4n8p)+(n,X)	RU119	(n,5n8p)+(n,X)	RU118
(n,6n8p)+(n,X)	RU117	(n,7n8p)+(n,X)	RU116
(n,8n8p)+(n,X)	RU115	(n,9n8p)+(n,X)	RU114
(n,10n8p)+(n,X)	RU113	(n,11n8p)+(n,X)	RU112
(n,12n8p)+(n,X)	RU111	(n,13n8p)+(n,X)	RU110
(n,14n8p)+(n,X)	RU109	(n,15n8p)+(n,X)	RU108

Appendix C

Table 9: List of materials for which neutron cross sections are available in FLUKA (taken from [55]). Evaluated libraries from which data are taken are indicated. Fourth and fifth columns give the availability of information on production of residual nuclei and gamma, respectively.

Material	Temperature	Origin	Nuclei production	Gamma production
H	293K	JEF-2.2	No	Yes
1H	293K	JEF-2.2	No	Yes
H	87K	JEF-2.2	No	Yes
2H	293K	JEF-1	No	Yes
3He	293K	JEF-1	Yes	No
He	293K	JEF-1	Yes	No
Li	293K	ENDF/B-VI	Yes	Yes
Li	87K	ENDF/B-VI	Yes	Yes
6Li	293K	ENDF/B-VI	Yes	Yes
6Li	87K	ENDF/B-VI	Yes	Yes
7Li	293K	ENDF/B-VI	Yes	Yes
7Li	87K	ENDF/B-VI	Yes	Yes
9Be	293K	ENDF/B-VI	Yes	Yes
B	293K	JEF-2.2	Yes	Yes
10B	293K	JEF-2.2	Yes	Yes
11B	293K	ENDF/B-VI	Yes	Yes
C	293K	ENDF/B6R8	Yes	Yes
C	87K	ENDF/B6R8	Yes	Yes
14N	293K	JEF-2.2	Yes	Yes
14N	87K	JEF-2.2	Yes	Yes
16O	293K	ENDF/B6R8	Yes	Yes
16O	87K	ENDF/B6R8	Yes	Yes
19F	293K	ENDF/B-VI	Yes	Yes
23Na	293K	JEF-2.2	Yes	Yes
Mg	293K	JENDL3.2	Yes	Yes
Mg	87K	JENDL3.2	Yes	Yes
27Al	293K	ENDF/B6R8	Yes	Yes
27Al	87K	ENDF/B6R8	Yes	Yes

27Al	4K	ENDF/B6R8	Yes	Yes
Si	293K	JENDL3.3	Yes	Yes
Si	87K	JENDL3.3	Yes	Yes
31P	293K	ENDF/B-VI	Yes	Yes
S	293K	JENDL3.2	Yes	Yes
Cl	293K	ENDF/B-VI	No	Yes
Ar	293K	ENDL	Yes	Yes
Ar	87K	ENDL	Yes	Yes
K	293K	ENDF/B-VI	Yes	Yes
K	87K	ENDF/B-VI	Yes	Yes
Ca	293K	JENDL-3.3	Yes	Yes
Ti	293K	JEF-2.2	Yes	Yes
V	293K	ENDF/B-VI	Yes	Yes
V	87K	ENDF/B-VI	Yes	Yes
Cr	293K	ENDF/B-VI	Yes	Yes
Cr	87K	ENDF/B-VI	Yes	Yes
55Mn	293K	ENDF/B-VI	Yes	Yes
55Mn	87K	ENDF/B-VI	Yes	Yes
Fe	293K	ENDF/B-VI	Yes	Yes
Fe	87K	ENDF/B-VI	Yes	Yes
59Co	293K	ENDF/B-VI	Yes	Yes
59Co	87K	ENDF/B-VI	Yes	Yes
Ni	293K	ENDF/B-VI	Yes	Yes
Ni	87K	ENDF/B-VI	Yes	Yes
Cu	293K	ENDF/B-VI	Yes	Yes
Cu	87K	ENDF/B-VI	Yes	Yes
Zn	293K	ENEA	No	Yes
Zn	87K	ENEA	No	Yes
Ga	293K	ENDF/B-VI	No	Yes
Ga	87K	ENDF/B-VI	No	Yes
Ge	293K	JEF-1	No	No
75As	293K	JEF-1	Yes	No
Br	293K	JENDL-3.2	Yes	No
Kr	293K	JEF-2.2	Yes	No
Kr	120K	JEF-2.2	Yes	No
90Sr	293K	JEF-2.2	Yes	No
Zr	293K	BROND	Yes	Yes
93Nb	293K	ENDF/B6R8	Yes	Yes

93Nb	87K	ENDF/B6R8	Yes	Yes
Mb	293K	EFF2.4	Yes	Yes
Mb	87K	EFF2.4	Yes	Yes
99Tc	293K	JEF-2.2	Yes	No
Ag	293K	JENDL-3.2	Yes	Yes
Cd	293K	JENDL-3	No	Yes
In	293K	JEF-1	Yes	No
Sn	293K	JENDL-3	Yes	No
Sn	87K	JENDL-3	Yes	No
Sb	293K	ENDF/B-VI	Yes	No
Sb	87K	ENDF/B-VI	Yes	No
127I	293K	JEF-2.2	Yes	No
129I	293K	JEF-2.2	Yes	No
Xe	293K	JEF-2.2	Yes	No
124Xe	93K	JEF-2.2	Yes	No
126Xe	293K	JEF-2.2	Yes	No
128Xe	293K	JEF-2.2	Yes	No
129Xe	293K	JEF-2.2	Yes	No
130Xe	293K	JEF-2.2	Yes	No
131Xe	293K	JEF-2.2	Yes	No
132Xe	293K	JEF-2.2	Yes	No
134Xe	293K	JEF-2.2	Yes	No
135Xe	293K	JEF-2.2	Yes	No
136Xe	293K	JEF-2.2	Yes	No
133Cs	293K	JEF-2.2	Yes	No
135Cs	293K	JEF-2.2	Yes	No
137Cs	293K	JEF-2.2	Yes	No
Ba	293K	JEF-1	Yes	No
Ce	293K	JEF-2.2	Yes	No
Sm	293K	ENDF/B6R8	Yes	No
Gd	293K	ENDF/B-VI	Yes	No
Gd	87K	ENDF/B-VI	Yes	No
181Ta	293K	ENDF/B6R8	Yes	Yes
181Ta	87K	ENDF/B6R8	Yes	Yes
W	293K	ENDF/B6R8	Yes	Yes
W	87K	ENDF/B6R8	Yes	Yes
186W	293K	ENDF/B6R8	Yes	Yes
Re	293K	ENDF/B-VI	Yes	No

Re	87K	ENDF/B-VI	Yes	No
197Au	293K	ENDF/B-VI	Yes	Yes
Hg	293K	JENDL-3.3	Yes	No
Pb	293K	ENDF/B6R6	Yes	Yes
208Pb	293K	ENDF/B6R6	Yes	Yes
Pb	87K	ENDF/B6R6	Yes	Yes
209Bi	293K	JEF-2.2	Yes	Yes
209Bi	87K	JEF-2.2	Yes	Yes
230Th	293K	ENDF/B-VI	Yes	No
232Th	293K	ENDF/B-VI	Yes	Yes
233U	293K	ENDF/B-VI	Yes	Yes
234U	293K	ENDF/B-VI	Yes	Yes
234U	87K	ENDF/B-VI	Yes	Yes
235U	293K	ENDF/B-VI	Yes	Yes
235U	87K	ENDF/B-VI	Yes	Yes
238U	293K	ENDF/B-VI	Yes	Yes
238U	87K	ENDF/B-VI	Yes	Yes
237Np	293K	ENDF/B-VI	Yes	Yes
239Pu	293K	ENDF/B-VI	Yes	Yes
239Pu	87K	ENDF/B-VI	Yes	Yes
241Am	293K	ENDF/B-VI	Yes	Yes
243Am	293K	ENDF/B-VI	Yes	Yes

References

- [1] Q. R. Ahmad *et al.*, *Phys. Rev. Lett.* **89** (2002) 001302 and references therein. Q. R. Ahmad *et al.*, *Phys. Rev. Lett.* **92** (2004) 181301.
- [2] S. Fukuda *et al.*, *Phys. Rev. Lett.* **86** (2001) 5656 and references therein. M. B. Smy *et al.*, *Phys. Rev.* **D69** (2004) 011104.
- [3] T. Kajita, Y. Totsuka, *Rev. Mod. Phys.* **73** (2001) 85 and references therein.
- [4] K. Eguchi *et al.*, *Phys. Rev. Lett.* **90** (2003) 021802.
- [5] F. Feruglio, A. Strumia, F. Vissani, *Nucl. Phys.* **B637** (2002) 345. F. Feruglio, A. Strumia, F. Vissani, *Nucl. Phys.* **B659** (2003) 359, Addendum, also references therein. S. Pascoli, S.T. Petkov, W. Rodejohann, *Phys. Lett.* **B558** (2003) 141. R. R. Joaquim, *Phys. Rev.* **D68** (2003) 033019.
- [6] S. Elliott, P. Vogel, *Annu. Rev. Nucl. Part. Sci.* **52** (2002) 115. A. Morales, J. Morales, *Nucl. Phys. (Proc. Suppl.)* **B114** (2003) 141. O. Cremonesi, *Nucl. Phys. (Proc. Suppl.)* **B118** (2003) 287.
- [7] O. Elgaroy *et al.*, *Phys. Rev. Lett.* **89** (2002) 061301.
- [8] V. M. Lobashov, *Nucl. Phys.* **A719** (2003) 153 and references therein.
- [9] G. F. Dell’Antonio, E. Fiorini, *Suppl. Nuovo Cimento* **17** (1960) 132.
- [10] H. V. Klapdor-Kleingrothaus, A. Dietz, H. L. Harney, I. V. Krivosheina, *Mod. Phys. Lett.* **A16** (2001) 2409.
- [11] C. E. Aalseth *et al.*, *Mod. Phys.* **A17** (2002) 1475. Yu. G. Zdesenko, F. A. Danevich, V. I. Tretyak, *Phys. Lett.* **B546** (2002) 206 and references therein.
- [12] A.M. Bakaliarov *et al.*, “Results of the Experiment on Investigation of Germanium-76 Double Beta Decay”, presented at NANP2003, Dubna, June 24, 2003, [arXiv:hep-ex/0309016].
- [13] H. V. Klapdor-Kleingrothaus *et al.*, *Phys. Lett.* **B586** (2004) 198.
- [14] G. Heusser, “Low-radioactivity background techniques”, *Annu. Rev. Nucl. Part. Sci.* **45** (1995) 543.
- [15] D. Lal and B. Peters, “Cosmic Ray Produced Radioactivity on the Earth”, Springer, Berlin, Heidelberg, 1967.
- [16] W.N. Hess, H. W. Patterson, R. Wallacew, *Phys. Rev.* **116** (1959) 449.
- [17] J. F. Ziegler, *Journal of Research and Development IBM*, **42** (1998) 1.

- [18] F. T. Avignone *et al.*, *Nucl. Instr. (Proc. Suppl.)* **B28A** (1992) 280.
- [19] Majorana Collaboration, “*White Paper on the Majorana zero-neutrino Double Beta Decay Experiment*”, [arXiv:nucl-ex/0311013].
- [20] CUORE Collaboration, “*CUORE: a Cryogenical Underground Observatory for Rare Events*”, CUORE Proposal, <http://crio.mib.infn.it/wig/>.
- [21] L. Baudis *et al.*, *Nucl. Instr. And Meth.* **A426** (1999) 425. GENIUS Collaboration, “*GENIUS: a supersensitive Germanium Detector System for Rare Events*”, [arXiv:hep-ph/9910205].
- [22] GERDA Collaboration, “*A new ^{76}Ge Double Beta Decay Experiment at Gran Sasso*”, GERDA Letter of Intent, <http://www.mpi-hd.mpg.de/ge76/home.html>, [arXiv.org: hep-ex/0404039].
- [23] C. Doerr, H. V. Klapdor-Kleingrothaus, *Nucl. Instr. And Meth* **A513** (2003) 596.
- [24] L. Baudis, R. W. Schnee, “*NUSL White Paper: Dark Matter experiments*”, <http://nucth.physics.wisc.edu/conferences/white/Homestake.html>.
- [25] <http://www-nds.iaea.or.at/exfor/>.
- [26] <http://www-nds.iaea.or.at/ndspub/rnal/www/>.
- [27] Yu.N. Shubin, V.P. Lunev, A.Yu. Konobeyev, A.I. Ditjuk, “*Cross-section data library MENDL-2 to study activation as transmutation of materials irradiated by nucleons of intermediate energies*”, report INDC(CCP)-385 (International Atomic Energy Agency, May 1995).
- [28] M. Blann, H.K. Vonach, *Phys. Rev.* **C28** (1983) 1475.
- [29] A. Iwamoto, K. Harada, *Phys. Rev.* **C26** (1982) 1821; N. Sato, A. Iwamoto, K. Harada, *Phys. Rev.* **C28** (1983) 1527.
- [30] A.V. Ignatyuk, G.N. Smirenkin, A.S.Tishin, *Yadernaya Fizika* **21** (1975) 485.
- [31] S. G. Mashnik, A. J. Sierk, K. A. Van Riper, W. B. Wilson. *Proc. Fourth Workshop on Simulating Accelerator Radiation Environments (SARE4)*, Knoxville, Tennessee, September 14–16, 1998. LANL Report LA-UR-98-6000 (1998), [arXiv.org:nucl-th/9812071].
- [32] K. A. Van Riper, S. G. Mashnik, W. B. Wilson, “*Study of Isotope Production in High Power Accelerators: Detailed Report*”, LA-UR-98-5379. K. A. Van Riper, S. G. Mashnik, W. B. Wilson, LA-UR-99-360, [arXiv.org:nucl-th/9901073].
- [33] A.S. Iljinov, V.G. Semenov, M.P. Semenova, N.M. Sobolevsky, L.V. Udovenko. “*Production of Radionuclides at Intermediate Energies*”, Springer Verlag, Landolt-Bornstein, New Series, subvolumes I/13a (1991), I/13b (1992), I/13c (1993), and I/13d (1994).

- [34] R. Silberberg and C. H. Tsao, *Ap. J. Suppl.* **35** (1977) 137.
- [35] R. Silberberg and C. H. Tsao, *Ap. J. Suppl.* **25** (1973) 315, *Ap. J. Suppl.* **25** (1973) 335.
- [36] C. J. Martoff, P. D. Lewin, *Comput. Phys. Commun.* **72** (1992) 96.
- [37] J. Bockholt, “Der Untergrund von angereicherten 70 Ge-Detektoren”, PhD thesis, University of Heidelberg, 1994.
- [38] R. Michel and P. Nagel, “*International Codes and Model Intercomparison for Intermediate Energy Activation Yields*”, NSC/DOC(97)-1, January 1997 <http://www.nea.fr/html/science/pt/ieay>.
- [39] S. G. Mashnik *et al.*, “*Cascade-exciton Model detail analysis of proton spallation at energies from 10 MeV to 5 GeV*”, <http://t2.lanl.gov/publications/CEM95/normal/report.ps>.
- [40] S. G. Mashnik *et al.*, *Proc. Int. Conf. on Nuclear Data for Science and Technology (ND2001)*, October 7–12, 2001, Tsukuba, Ibaraki, Japan, LA-UR-01-5391, [arXiv:nucl-th/0208075].
- [41] Yu. E. Titarenko *et al.*, *Proc. of 3rd Topical Meeting on Nuclear Applications of Accelerators Technology (AccApp'99)*, ANS 1999 Winter Meeting, Long Beach, CA, November 14-18, 1999, LA-UR-99-4489, [arXiv:nucl-ex/9908012].
- [42] Yu. E. Titarenko *et al.*, *Proc. of Workshop on Nuclear Data for the Transmutation of Nuclear Waste (TRAMU)*, GSI, Darmstadt, Germany, September 2–5, 2003, LA-UR-04-0366, [arXiv:nucl-ex/0401034].
- [43] R. Silberberg and C. H. Tsao, *Ap. J. Suppl.* **35** (1977) 129, *Ap. J. Suppl.* **58** (1985) 873, *Phys. Rep.* **191** (1980) 351.
- [44] R. Silberberg and C. H. Tsao, *Ap. J.* **501** (1998) 911.
- [45] G. Rudstam, *Z. Naturforschung* **A21** (1966) 1027.
- [46] Y. Ramachers, “*Background considerations for CRESST. Cosmic activation*”, Private communication.
- [47] T. W. Armstrong, K. Chandler, J. Barish, *J. Geophys. Res.* **78** (1973) 2715.
- [48] S. Agostinelli *et al.*, *Nucl. Instr. and Meth. A* **506** (2003)250, <http://www.cern.ch/geant4>.
- [49] GEANT4 Collaboration, “*Physics reference manual*”.
- [50] J. P. Wellisch, *Proc. of Computing in High Energy and Nuclear Physics*, La Jolla, California, March 24–28, 2003 , [arXiv.org:nucl-th/0306006].
- [51] GEANT4 Collaboration, “*GEANT4 User's guide: for Toolkit Developers*”.

- [52] J. P. Wellisch, “*Neutron induced isotope production on selected CMS elements using GEANT4*”, CMS Note 1999/070.
- [53] G. Folger, J.P. Wellisch, *Proc. of Computing in High Energy and Nuclear Physics*, La Jolla, California, March 24–28, 2003, [arXiv.org:nucl-th/0306007].
- [54] A. Heikkinen, N. Stepanov, J.P. Wellisch, *Proc. of Computing in High Energy and Nuclear Physics*, La Jolla, California, March 24–28, 2003, [arXiv.org:nucl-th/0306008]. V. Ivanchenko, G. Folger, J.P. Wellisch, T. Koi, D.H. Wright, *Proc. of Computing in High Energy and Nuclear Physics (CHEP03)*, La Jolla, Ca, USA, March 2003, [arXiv.org:nucl-th/0306016].
- [55] A. Fassò, A. Ferrari, P.R. Sala, “*Electron-photon transport in FLUKA: status*”, *Proceedings of the MonteCarlo 2000 Conference*, Lisbon, October 23–26 2000, edited by A. Kling, F. Barao, M. Nakagawa, L. Tavora, P. Vaz, Springer-Verlag Berlin, p.159–164 (2001). A. Fassò, A. Ferrari, J. Ranft, P.R. Sala, “*FLUKA: Status and Prospective for Hadronic Applications*”, *ibid*, p.955–960 (2001). <http://www.fluka.org>.
- [56] A. Fassò et al, *Proc. of Computing in High Energy and Nuclear Physics (CHEP03)*, La Jolla, California, [arXiv:hep-ph/0306267].